Elastic Scattering of Alpha Particles by Carbon-14*

JAMES A. WEINMAN AND EDWARD A. SILVERSTEIN
University of Wisconsin, Madison, Wisconsin

(Received January 23, 1958)

The elastic scattering of alpha particles by C^{14} has been observed for alpha energies between 2.0 and 3.9 Mev and for $\theta_{c.m.}=169°$, 149.5°, 140.8°, 125.3°, and 90°. The solid targets of 38.6% C^{14} were at least 8 kev thick. Energies of both the incident and scattered particles were measured with cylindrical electrostatic analyzers. The off-resonance cross sections were normalized to those derived from dispersion theory. Dispersion formalism applied to $C^{14}(\alpha,\alpha)C^{14}$ and $C^{14}(\alpha,n)O^{17}$ data yields the resonance energies, angular momenta, parities, and reduced widths of several O^{18} levels. The levels of O^{18} considered had the following resonant energies, parities, and J values: 8.051 Mev (0^+ or 1^-), 8.222 Mev (2^+), 8.293 Mev (3^-), 8.966 Mev ($\geq 2^+$), and 9.0 to 9.2 Mev two levels, either (2^+3^-) or (4^+3^-).

INTRODUCTION

THE $C^{14}(\alpha,\alpha)C^{14}$ reaction creates an O^{18} compound nucleus excited to an energy of 6.238 Mev.[1] By bombarding the C^{14} nucleus with alpha particles from 2 to 4 Mev, information was obtained about the excited states of O^{18} in the energy range of 7.79 to 9.35 Mev.

By combining the data from the $C^{14}(\alpha,\alpha)C^{14}$ reaction with the data from the $C^{14}(\alpha,n)O^{17}$ reaction,[2] energy levels of the compound nucleus were located; in some instances the width of the levels, the angular momentum values, and the parity of the levels were measured or inferred. The reduced widths of these O^{18}* levels were also calculated when sufficient data were available. Since both the alpha particle and the carbon-14 nucleus have zero spin,[3] the reaction is readily amenable to analysis by dispersion theory.[4] Conservation of angular momentum and parity make it impossible for the combination of an alpha particle and a C^{14} nucleus (both of which have zero-spin and even-parity ground states) to form an excited state of O^{18} that has odd angular momentum and even parity or vice versa.

APPARATUS AND PROCEDURE

The entire apparatus used in this experiment is shown schematically in Fig. 1.

The beam of singly-ionized alpha particles from an electrostatic generator was deflected by a magnetic analyzer to separate beam components of differing momenta, and by a cylindrical electrostatic analyzer for precision energy measurement. The energy resolution of the beam incident on the target was determined by means of adjustable slit widths to about $\pm 0.05\%$ for this experiment.

The target material supplied to us by the Oak Ridge National Laboratory was a mixture of 38.6% C^{14}, 0.6% C^{13}, and 61.4% C^{12}. In view of the expense of this isotope mixture, solid targets were used.

The procedure for preparation of C^{14} targets has already been described by Douglas.[5] It was desirable to use a target backing of lower atomic mass than 14 so that alpha particles scattered from C^{14} would be the most energetic ones present for a given incident energy. Ordinary carbon (99% C^{12}) is satisfactory. The backings were made of carbon black[6] pressed inside 1.2-cm diam $\times$0.6-cm deep stainless steel cylinders under a force of 2000 pounds. The front face of the pellet which was to be covered with the C^{14} was pressed against a piece of glass to give a smooth surface. The resultant pellet was then heated under vacuum to drive away vapors adsorbed on the carbon black. The C^{14} was deposited on the faces of the pellets which formed the two plane electrode surfaces for a high-frequency discharge.[5] The thickness of the deposit on the backing was found from the experimental width of the 2642-kev level whose natural width is 10 kev.[2]

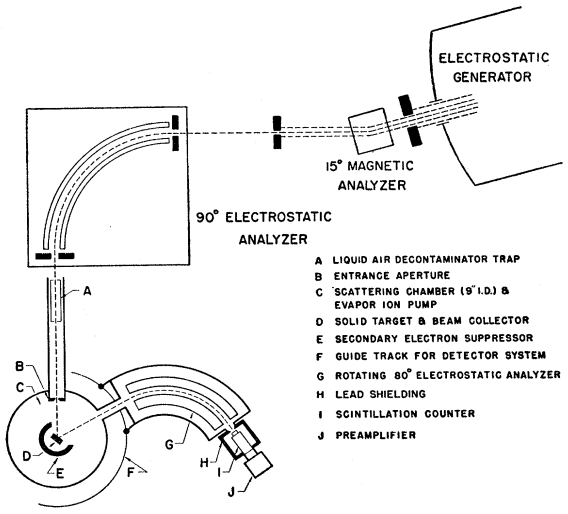

FIG. 1. Schematic diagram of apparatus.

* Work supported by the U. S. Atomic Energy Commission, and by the Graduate School from funds supplied by the Wisconsin Alumni Research Foundation.

[1] F. Ajzenberg and T. Lauritsen, Revs. Modern Phys. **27**, 142 (1955).
[2] R. M. Sanders, Phys. Rev. **104**, 1434 (1956).
[3] J. E. Mack, Revs. Modern Phys. **22**, 64 (1950).
[4] R. G. Sachs, *Nuclear Theory* (Addison-Wesley Press, Cambridge, 1953).
[5] Douglas, Gasten, and Mukerji, Can. J. Phys. **34**, 1097 (1956).
[6] Godfrey L. Cabot, Inc., 77 Franklin St., Boston, Massachusetts. Type: "Monarch 80." Particle diameter: 2000 A.

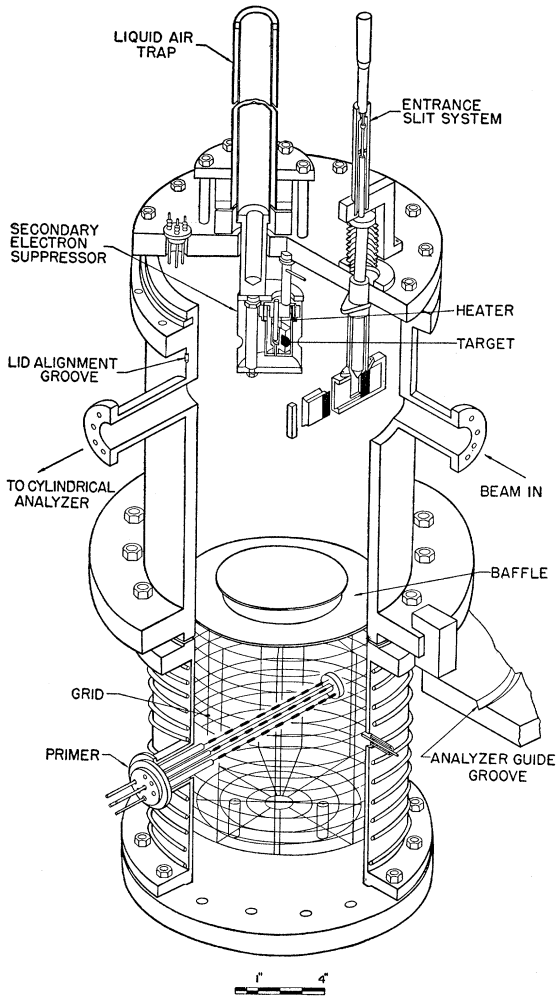

FIG. 2. Scattering chamber and Evapor-Ion pump.

Scattering Chamber

The scattering chamber and associated pump are shown in Fig. 2.

In order to assure that no extraneous C^{12} from organic vapors covered the target, the following precautions were taken:

The entire scattering chamber and detector system was isolated from the generator and its electrostatic analyzer by means of a cold trap.[2,7]

The scattering chamber and electrostatic analyzer were constructed of metal and ceramic components. These were also capable of being baked for outgassing.

The chamber was pumped by a modified Evapor-Ion[8] pump. This pump was merely a water-cooled enclosure which housed a battery of six tungsten rods (designated as "primer" in Fig. 2) 0.040 in. in diameter×7 in. long; these rods were wrapped with 0.020-in. diameter titanium wire. Upon passage of a current of about 60 amperes through one of these rods, the titanium evaporated, thus gettering the chamber. By continuing to pass about 45 amperes through the tungsten rods and applying 1500 volts ac to a grid which surrounded these tungsten rods, a sufficient number of electrons was extracted from the rods to ion-pump the entire system down to 5×10^{-7} mm of Hg.

The target was held at about 100°C by means of a small nichrome heater in the target holder. The target temperature was determined by a copper-constantan thermocouple embedded in the target holder.

The secondary electron suppressor which surrounded the target was maintained at liquid air temperatures to reduce still further the possibility of target contamination. The electron suppressor was maintained at -250 volts with respect to ground.

A variable entrance aperture was used to define the size of the beam and hence determine the resolution of the detector system. The target holder, suppressor, and slits were suspended from the lid of the scattering chamber for ease of removal and maintenance.

Cylindrical Electrostatic Analyzer

The primary consideration in the design of the particle detector system was to separate alpha particles scattered elastically by C^{14} from those scattered by C^{12}. An alpha particle of mass m_α, scattered elastically from a nucleus of mass M through an angle θ in the laboratory system, will have an energy in the laboratory system given by the expression

$$E_{\text{out}}^{\text{lab}}=K(M,\theta)E_{\text{in}}^{\text{lab}},$$

where

$$K(M,\theta)=\left\{\cos\theta+\left[\cos^2\theta+\left(\frac{M}{m_\alpha}\right)^2-1\right]^{\frac{1}{2}}\right\}^2\Big/\left(1+\frac{M}{m_\alpha}\right)^2.$$

The resolution of the detector ($\delta E/E$) must be less than $[K(14,\theta)-K(12,\theta)]/K(14,\theta)$, where θ is taken as the maximum forward angle used.

Accordingly, the most stringent requirement is a resolution of 0.072 or better for adequate separation at $\theta=74.1°$ (90° c.m.) of the alpha particles scattered from C^{14} from those scattered from C^{12}. To achieve this resolution, the cylindrical electrostatic analyzer shown in Fig. 3 was constructed. The parameters[9] characterizing this analyzer are shown in Table I.

The plates were made of highly polished cold-rolled steel; these were insulated by four steatite standoffs. The entire structure was of metal and ceramic except for the O-ring which held the scintillation counter.

The power supply used with this analyzer, although

[7] G. H. Miller, Rev. Sci. Instr. **24**, 549 (1953).

[8] *Vacuum Symposium Transactions* (Committe on Vacuum Techniques, Box 1282, Boston, Massachusetts, 1955), p. 83ff.

[9] Warren, Powell, and Herb, Rev. Sci. Instr. **18**, 559 (1947).

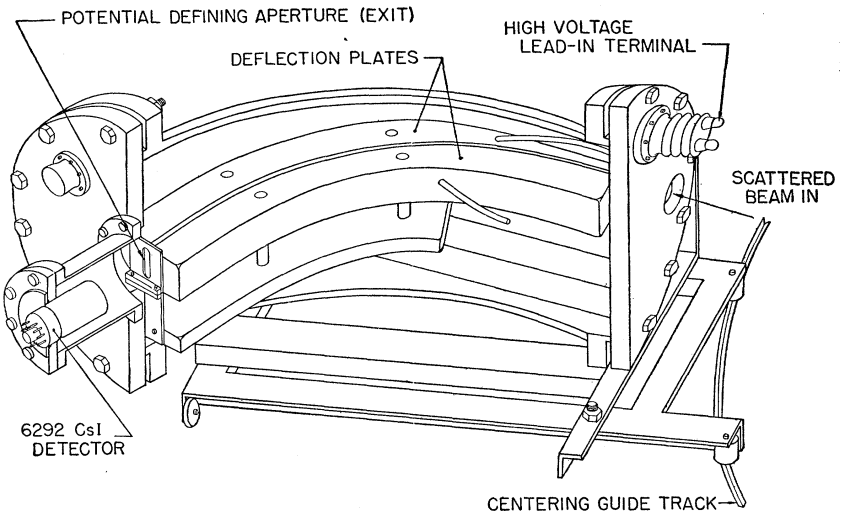

FIG. 3. Cylindrical electrostatic analyzer used to separate alpha particles scattered by C^{14} from those scattered by C^{12}.

modified, was essentially similar to the one described by Henkel and Petree.[10]

Detector System

The electrostatic analyzer for the reaction products passed He^{++} ions with energy E and He^{+} ions with energy $\frac{1}{2}E$ for the same voltage settings. Since both ions were always present, the final detector must separate these two groups of ions. A scintillation counter was used to obtain the 30% energy resolution required to obtain clear separation of the groups. The counter utilized in this experiment was a crystal of CsI(Tl) 1.2 cm×1.2 cm×0.005 cm.

A cylindrical shell of lead 5 cm thick which was mounted coaxially with the scintillation counter was used to shield the counter against the x-ray background in the experimental area.

EXPERIMENTAL RESULTS AND DISCUSSION OF ERRORS

Cross-Section Measurements

The yield of He^{++} ions was measured in the energy range of 2 to 4 Mev for the back angle (169°) and the angles (149.5°, 140.8°, 125.3°, and 90°) corresponding to zeros of Legendre polynomials of orders $l=4$, 3, 2, and 1, respectively, in the center-of-mass system for incident alpha particles. Four scattering anomalies were observed in this range. Figure 4 shows the differential cross section in the center-of-mass system as a function of the energy of the incident alpha particles.

TABLE I. Cylindrical electrostatic analyzer parameters.[a]

Radius of median trajectory	39.69 cm
Angle subtended by plates, ϕ	80°
Separation of plates	0.63 cm
Approximate cross section of plates	4.44 cm×4.44 cm
Voltage	−20 to +20 kv
Maximum energy α^{++} particle analyzed	2.5 Mev
Solid angle subtended by 1.27 cm×4.45 cm detector (steradians)	6×10^{-4}
Magnification	0.65
f (focal length)	30.48 cm
l' (object to analyzer entrance distance)	35.56 cm
l'' (image to analyzer exit distance)	7.87 cm
$g(l'-g)(l''-g)=f^2$	−11.83 cm

[a] See reference 9.

Effective target thicknesses were found to be approximately 10 kev or more. The experimental points were taken at 10-kev intervals at $\theta_{c.m.}=169°$, and closer whenever a resonance in the cross section was encountered. At other angles the energy interval chosen between points was dependent on the behavior of the 169° cross section. Figure 5 shows the energy distribution of the scattered alpha particles for $\theta_{lab}=74.1°$ and $\theta_{lab}=165°$. The rise at low energy corresponds to scattering from C^{12} (target and backing) while the high-energy peak is from C^{14}. Background under the C^{14} peak was assumed to interpolate linearly as indicated by the dotted line of Fig. 5. The background counts were most numerous at $\theta_{c.m.}=90°$; hence statistical errors were greatest there.

The yield was then corrected to account for the equilibrium fraction of He^{+} and He^{0} which emerged from the target and was not measured.[11] Dissanaike quotes an accuracy of 5%; however, these data were difficult to plot to that accuracy. Earlier workers quote 10% errors in the ratios He^{++}/He^{+} and He^{+}/He^{0}. Therefore a 10% error may be justified in the quantity He^{total}/He^{++} shown in Fig. 6. Although carbon was not one of the materials studied, the charge-exchange equilibrium data seemed independent of the material used as a target; this may have been due to thin carbon films that covered the targets considered. Charge-exchange corrections are most significant at $\theta_{c.m.}=169°$ at low energy where $He^{total}/He^{++}\cong 2$.

[10] R. L. Henkel and B. Petree, Rev. Sci. Instr. **20**, 729 (1949).

[11] G. Dissanaike, Phil. Mag. **44**, 1057 (1953); S. K. Allison and S. D. Warshaw, Revs. Modern Phys. **25**, 779 (1953).

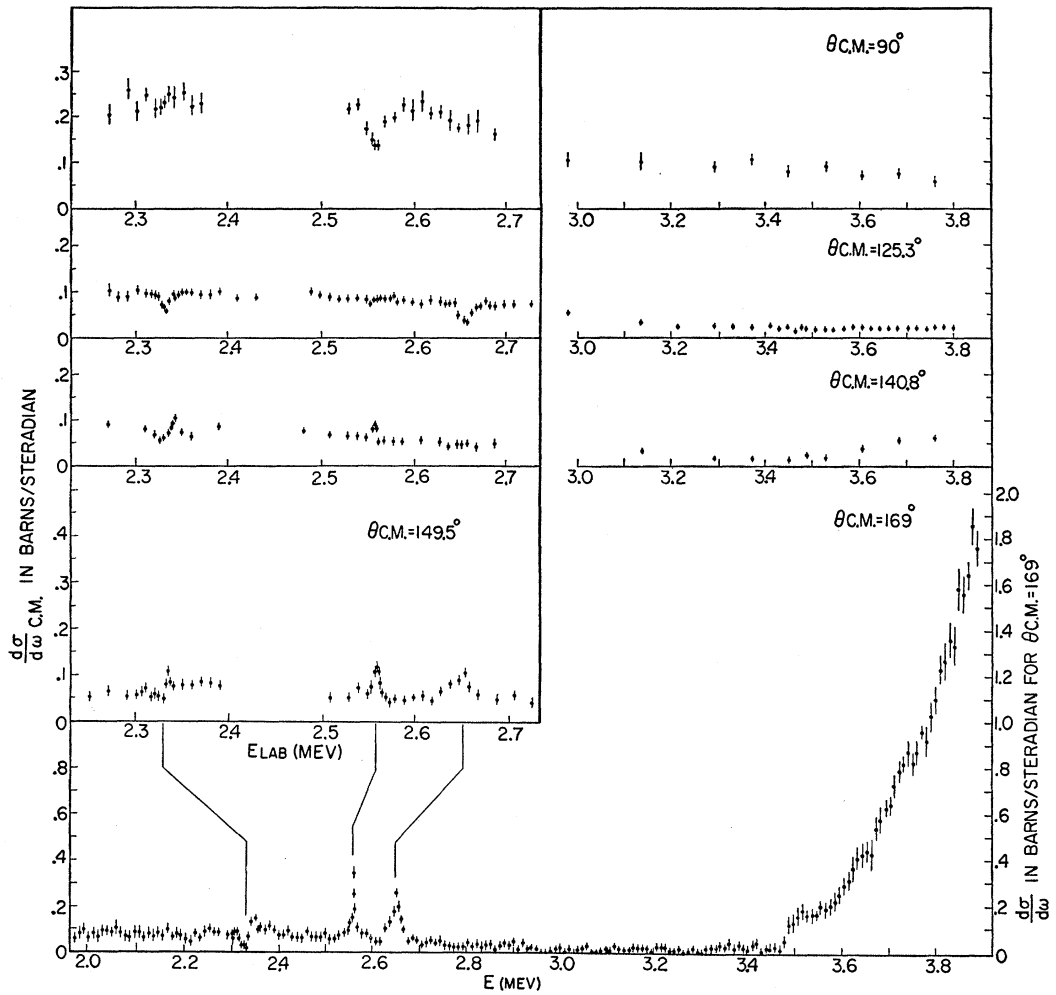

FIG. 4. Differential cross sections in the center-of-mass system as a function of the laboratory energy of the incident alpha particles. The ordinates are fixed by normalizing the nonresonant low-energy yield (after charge-exchange correction) to Rutherford plus hard-sphere cross sections.

This corrected yield, for energies away from anomalies, was then normalized by the method of least squares to an analytically derived cross section deduced from Rutherford and hard-sphere scattering assumptions.

Energy Measurement

The scattered-particle analyzer was calibrated by taking curves such as those in Fig. 5 at an incident alpha-particle energy that assured a large yield of alpha particles scattered from C^{14}. The scattered-particle analyzer potentiometer setting was plotted against the potentiometer setting of the incident-particle analyzer when the alpha-particle yield was a maximum. This linear relationship determined the scattered-beam analyzer potentiometer settings for all other incident energy settings except those occasional runs which were made to determine the background around the C^{14} peak. The energy of the scattered alpha particles was determined within $\pm 1\%$.

No precision calibration of the incident alpha energy was performed, since Sanders had already determined the resonant energies accurately in terms of the $Li^7(p,n)Be^7$ threshold. The only exception to this is the $E_r=2.331$-Mev resonance (which is below the $C^{14}(\alpha,n)O^{17}$ threshold), whose energy was derived from the 2.553-Mev resonance by

$$E_r=(2.553+\tfrac{1}{2}T)(X_1/X_2)-\tfrac{1}{2}T,$$

where X_1 and X_2 are potentiometer settings on the incident-beam electrostatic analyzer control corresponding to the resonant energies of the two resonances under consideration. (The choice of these X's depends on the analytically derived resonance shape as a function of energy.) T is the thickness of the particular target used for both X_i determinations.

Separation of He^{++} from He^{+} by the scintillation detector gave rise to an uncertainty of 9% at the back angle observation before pains were taken to improve

TABLE II. Summary of resonance parameters.

E_r(lab) (Mev)	O^{18*} (Mev)	J^π	Total width Γ_{lab} (kev)	$\Gamma_{\alpha\,c.m.}$ (kev)	$\gamma_{\lambda\alpha}^2$ c.m. (10^{-13} Mev cm)	% Single-particle width ($3\hbar^2/2\mu a$)	$\Gamma_{n\,c.m.}$ (kev)	γ_{n}^2 c.m. (10^{-17} Mev cm)	% Single-particle width ($3\hbar^2/2\mu a$)
2.331±5	8.051	0^+ or 1^- [b]	<6 ±3	<5 ±2	<0.1	<2.8	...	...	...
2.553±4[a]	8.222	2^+	1.6±1[a]	1.2±0.8	0.032	0.90	0.014±0.009	0.82	6.2×10^{-4}
2.642±5[a]	8.293	3^-	10 ±1[a]	6.9±0.4	0.72	20	0.83 ±0.49	210	0.16
2.798±11[a]	8.412	...	22 ±10[c]	...	...	...	...	...	...
3.336±20[a]	8.830	...	100 ±20[c]	...	...	...	...	...	...
3.508±5[a]	8.966	$\geq 2^+$	54 ±5[a]	...	...	...	...	...	...
3.6 to 3.9	9.0 to 9.2	(2^+3^-) or (4^+3^-)	...	...	...	...	...	...	...

[a] Quantities obtained from $C^{14}(\alpha,n)O^{17}$ data.
[b] Recent work on $C^{14}(\alpha,\gamma)O^{18}$ fixes this level as 1^- [W. R. Phillips (to be published)].
[c] Quantities obtained from $C^{14}(\alpha,n)O^{17}$ but not clearly observed in $C^{14}(\alpha,\alpha)C^{14}$.

the scintillator resolution. Once the scintillation counter resolution was improved, the uncertainty from this factor was reduced to 2%, and all yields at angles other than $\theta_{c.m.}=169°$ were observed in this improved manner.

The thickness and condition of the target surface also influence the resolution of the measurements.[2] Occasional checks were made on the shape of the resonance at 2.56 Mev when the condition of the target was in doubt. Flaking of the target limited the incident current density to approximately 1 μa/cm^2.

DISCUSSION OF RESULTS

Parameters can be assigned to the levels in O^{18} under consideration by combining information derived from the elastic alpha-scattering differential cross section with information from the $C^{14}(\alpha,n)O^{17}$ reaction.[2] These parameters are summarized in Table II. Certain of these assignments are discussed in more detail below.

A. The 2.331-Mev Resonance

The presence of the resonance at all angles except perhaps 90° c.m. implies P-wave formation and hence $J^\pi=1^-$. However the data at 90° c.m. are not good enough to exclude an interference dip such as would arise from S-wave alpha particles. An attempt was therefore made to distinguish between these two assignments by comparing the quantitative behavior of the cross-section curves at the various angles with the cross sections predicted by the dispersion theory.

The quantum-mechanical expression for the elastic scattering of alpha particles by C^{14} (spinless particles on spinless nuclei) is given in the one-level approximation by[4]:

$$\frac{d\sigma}{d\omega}=k^{-2}\left|-\frac{\alpha}{2}\csc^2\left(\frac{\theta}{2}\right)\exp\left[i\alpha\ln\csc^2\left(\frac{\theta}{2}\right)\right]+\sum_{l=0}^{\infty}(2l+1)e^{2i(\eta_l-\eta_0)}\left\{\frac{\Gamma_{\lambda\alpha l}}{\Gamma_\lambda}\sin(2\zeta)e^{2i\zeta}\times e^{2i\zeta_l}+e^{i\zeta_l}\sin\zeta_l\right\}P_l(\cos\theta)\right|^2.$$

Here k is the relative wave number; $\alpha=Z'Z''e^2M/\hbar^2k$, where Z' and Z'' are the charges of the target and projectile and M is the reduced mass of the alpha-C^{14} system; θ is the center-of-mass scattering angle;

$$e^{2i(\eta_l-\eta_0)}=\prod_{t=1}^{l}\left(\frac{t+i\alpha}{t-i\alpha}\right);$$

$\Gamma_{\lambda\alpha l}$ is the partial width for alphas from the level E_λ of the compound nucleus; and $\Gamma_\lambda=\sum_s\Gamma_{\lambda s}$, where s runs over all open channels.

The resonant phase shift is

$$\zeta=\tfrac{1}{2}\tan^{-1}[\tfrac{1}{2}\Gamma_\lambda/(E_\lambda'-E)].$$

Here $E_\lambda'=E_\lambda+\frac{1}{2}\sum_s Q_{\lambda,ss}\Gamma_{\lambda s}$, where $Q_{\lambda,ss}=-F_s(a_{0s})/G_s(a_{0s})$, with F_s and G_s defined in reference 4.

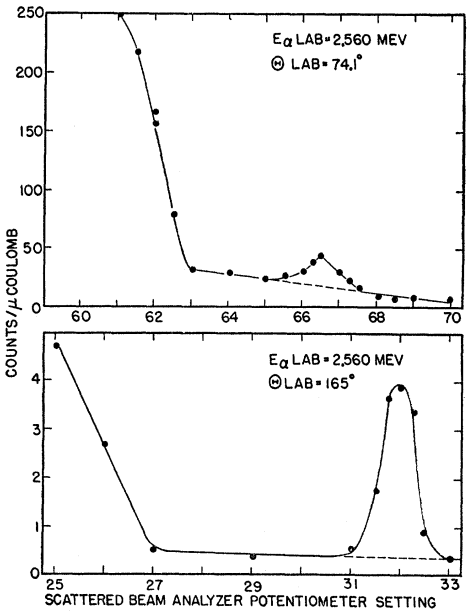

FIG. 5. Energy distribution of the alpha particles scattered from the target and backing. The small peak is from C^{14}, and the large low-energy rise is from the C^{12} in the target and backing. It can be seen how the difficulty of separation increases at the forward angle.

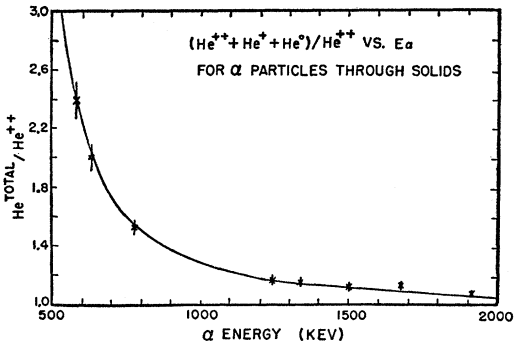

FIG. 6. Charge-exchange correction applied to yield of alphas emerging from target to give total alpha yield from the observed He^{++}. The solid line is Dissanaike's curve; the points are from Allision with the quoted errors indicated by the bars.

The potential phase shift is $\zeta_l=\tan^{-1}Q_{\lambda,ll}$, with $Q_{\lambda,ll}=-F_l(a_{0l})/G_l(a_{0l})$. F_l and G_l are the regular and irregular Coulomb functions defined in reference 4.[12] A convenient tabulation of the Coulomb functions is given by Sharp, Gove, and Paul.[13]

The reduced widths may be expressed as:

$$\gamma_{\lambda s}^2=\frac{\hbar}{2M_s}\Gamma_{\lambda s}[F_s^2+G_s^2].$$

Since this resonance is below the neutron threshold, we have $\Gamma_n=0$ and $\Gamma_\alpha=\Gamma$. at $\theta_{\text{c.m.}}=90°$, the above expression gives for an $l=0$ resonance $[(d\sigma/d\omega)_{\max}]^{\frac{1}{2}}-[(d\sigma/d\omega)_{\min}]^{\frac{1}{2}}=0.2$ (barn/sterad)$^{\frac{1}{2}}$, which is a larger variation than the observed value of 0.06 (barn/sterad)$^{\frac{1}{2}}$ (see Fig. 4). However, the observed width (15 kev) of this resonance is nearly that expected from instrumental effects (chiefly the target thickness of 12 kev). If the instrumental smearing reduced the expected S-wave amplitude variation by as much as a factor of three, the resultant 0.06 (barn/sterad)$^{\frac{1}{2}}$ dip would lie within the scatter of the experimental data. Unfortunately the cross-section uncertainties even at the other angles are large enough, and the qualitative behavior of an S and P resonance are similar enough, that no more definite assignment was possible.[14]

If the C^{14} target is uniform, then one can estimate the level width Γ from the observed width W and target thickness T by $W^2=T^2+\Gamma^2$. However, Sanders[2] found inconsistencies in this method for narrow resonances which he attributed to C^{14} target nonuniformity.[15] Since the present targets were made by the same method, possible target nonuniformity must be considered. (The thickness T was derived from the 2.642-Mev resonance where the effect of target nonuniformity is small.) The reduced width quoted in Table II is not sensitive to the ambiguity in S- or P-wave assignment since the S- and P-wave penetrabilities for this alpha energy are nearly the same.

[12] As mentioned in reference 4, these functions differ from the usual tabulated functions by a factor of $(M_s/\hbar k)^{\frac{1}{2}}$.

[13] Sharp, Gove, and Paul, Atomic Energy of Canada Limited Report AECL-268, Chalk River, Ontario (unpublished).

[14] Recent work on $C^{14}(\alpha,\gamma)O^{18}$ fixes this level as 1^- [W. R. Phillips (to be published)].

[15] An alternate explanation of his inconsistencies is that the asymmetry observed in the narrow resonance is a real nuclear effect resulting from interference with a weak broad level.

B. 2.553-Mev Anomaly

By virtue of its disappearance at $\theta_{\text{c.m.}}=125.3°$ and existence at all other angles, the anomaly must be attributed to a $J^\pi=2^+$ resonance. The 2.553-Mev resonance was observed from the $C^{14}(\alpha,n)O^{17}$ work[2] to have a width in the laboratory system of $\Gamma=1.6\pm1$ kev. The value of Γ found from Fig. 4 lies within the limits quoted by Sanders. From the relative yields of alpha particles and neutrons, we obtain

$$\Gamma\simeq\Gamma_\alpha\gg\Gamma_n.$$

For this $J^\pi=2^+$ resonance, outgoing $l=0$, 2, or 4 neutrons are permitted for the transition to the $J=\frac{5}{2}^+$ ground state of O^{17}. Since the available neutron energy in the c.m. system is but 152 kev, only S-wave (hence isotropic) neutron emission need be considered. Therefore Sanders' forward-angle data[16] imply a total (α,n) cross section at resonance of 24 ± 16 millibarns and yield the Γ_n and Γ_α of Table II.

C. The 2.642-Mev Anomaly

The disappearance of the resonance at $\theta_{\text{c.m.}}=90°$ and at 140.8° requires F waves and hence $J^\pi=3^-$. This result is also consistent with Sanders' (α,n) data[2] which required a $J=1^-$ or 3^- resonance. The present angular momentum assignment also permits the calculation of the neutron and alpha widths, as shown in Table II. (The large centripetal barrier for the 217-kev neutrons with $l=3$ implies that only $l=1$ neutrons need be considered.)

D. The 2.798-Mev Anomaly

The weak 2.798-Mev resonance in the (α,n) yield reported by Sanders[2] was not detected in the present $C^{14}(\alpha,\alpha)C^{14}$ data. Therefore $\Gamma_\alpha\ll\Gamma_n$ and $\Gamma_n\approx\Gamma\approx22\pm10$ kev. Hence the outgoing neutrons must have $l\lesssim2$ to comply with the Wigner limit on reduced widths.

E. The 3.336-Mev Anomaly

At $\theta_{\text{c.m.}}=169°$ there is perhaps a variation of ~30 mb/sterad in cross section which may be associated with an (α,n) resonance seen by Sanders at $E_\alpha=3.36$ Mev. The observed width is also consistent with the 100 kev quoted by him. The small effect of this resonance on the alpha scattering again implies $\Gamma_\alpha\ll\Gamma_n$ and $\Gamma_n\approx\Gamma\approx100$ kev. For such a case the Wigner limit restricts the outgoing neutrons to $l\lesssim2$.

[16] Corrected for the "peaking effect" of an assumed nonuniform C^{14} target.

F. The 3.508-Mev Anomaly

A resonance that corresponds to the 3.508-Mev, $C^{14}(\alpha,n)O^{17}$ resonance was observed at $\theta_{c.m.}=169°$. The observed width in the laboratory system is consistent with the 54 ± 5 kev value quoted by Sanders.[2] The cross-section variation at $\theta_{c.m.}=169°$ is about 170 ± 30 mb/sterad. This value is about seven times the maximum possible for an S-wave alpha-particle resonance but comparable to that expected for a P-wave resonance if $\Gamma_\alpha/\Gamma\approx1$. The $\theta_{c.m.}=140.8°$ data, however, argue against P-wave alphas since the cross-section variation should be down only a factor of two from the back-angle value. Figure 4 shows less than 20 mb/sterad variation at $\theta_{c.m.}=140.8°$ and $E_\alpha\approx3.51$ Mev. The large neutron yield from this resonance[2] is also in contradiction to our assumption of $\Gamma_\alpha/\Gamma\approx1$ which is necessary if P-wave alphas are involved. Formation by D-wave alphas (hence $J=2^+$) and a large Γ_n are consistent with all the alpha scattering data, and also with (α,n) data since S-wave neutrons could then be emitted. However, larger J values cannot be excluded.

G. The 3.8-Mev Anomaly

If a single resonance is to account for the rise in the $C^{14}(\alpha,\alpha)C^{14}$ cross section at $\theta_{c.m.}=169°$ above 3.6 Mev, then the magnitude of the anomaly implies that $l\geqslant4$ and $\Gamma_\alpha\approx\Gamma$ if $l=4$. The Wigner limit on the reduced alpha width for an $l=4$ resonance limits Γ_{lab} to 100 kev. However, Γ_{lab} is observed to be more than 200 kev. Therefore at least two overlapping resonances must be responsible for the observed anomaly.

Fifteen two-level combinations ($l\leqslant4$) are possible; however all but the (2^+3^-) and (4^+3^-) combinations can be eliminated. The arguments for acceptance or rejection of the various combinations are summarized in Table III.

TABLE III. Summary of the combinations of two levels which were tried in the attempt at fitting the anomaly at $E_\alpha>3.6$ Mev.

	0^+	1^-	2^+	3^-	4^+
4^+	a	a	b	Possible	c,e
3^-	d	d	Possible	d,e	
2^+	d	d	d,e		
1^-	d	d,e			
0^+	d,e				

[a] The Wigner limit implies $\Gamma_\alpha\leqslant100$ kev for the $l=4$ resonance; therefore the differential cross section below 3.7 Mev must be mainly due to the resonance in the S or P partial waves. However, at $\theta_{c.m.}=169°$ neither is sufficient to account for the cross section at $E_\alpha\leqslant3.7$ Mev.
[b] At $\theta_{c.m.}=125°$, where $P_2(\cos125°)=0$, this configuration predicts that the cross section will rise with increasing energy because of the $l=4$ resonance. This effect is not evident.
[c] Observed Γ_{lab} exceeds that allowed for the Wigner limit on $(\gamma_{\lambda\alpha})^2$.
[d] The maximum allowed differential cross section at $\theta_{c.m.}=169°$ is too small.
[e] Two levels of the same J and parity would produce a double peak.

The maximum possible value for $d\sigma/d\omega$ at $\theta_{c.m.}=169°$ is 2.85 barns/sterad if one assumes the (4^+3^-) combination. It is also possible to reproduce a constant differential cross section at $\theta_{c.m.}=125°$ by proper choice of the resonance energies.

For the (2^+3^-) combination the maximum possible value for $d\sigma/d\omega$ at $\theta_{c.m.}=169°$ is 1.95 barns/sterad. Again at $\theta_{c.m.}=125°$ a constant differential cross section can be obtained.

ACKNOWLEDGMENTS

The authors thank Professor H. T. Richards for his suggestion of the problem, and his guidance; Mr. Leroy Scharnke and other personnel of the shop for their helpful suggestions in the design and the machine work on the equipment described herein; and Ren Chiba, for his assistance in taking data. They also thank Dr. Willy Haeberli, Dr. David F. Herring, and Dr. Rod B. Walton for several helpful discussions.